Neural Schrödinger Bridge for Minimum Effort Stochastic Control of Colloidal Self-assembly

Abhishek Halder

Department of Applied Mathematics
University of California, Santa Cruz
Santa Cruz, CA 95064

Joint work with

Iman Nodozi
(UC Santa Cruz)

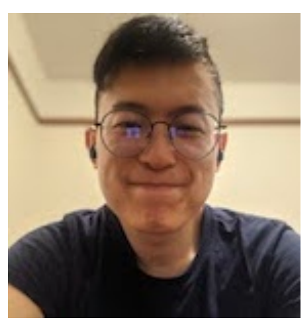

Charlie Yan
(UC Santa Cruz)

Mira Khare
(UC Berkeley)

Jared O'Leary
(UC Berkeley)

Ali Mesbah
(UC Berkeley)

Mini-symposium on Optimal Transport: Theory and Applications in Systems and Control
SIAM Conference on Control and Its Applications, Philadelphia
July 25, 2023

Colloidal Self-assembly (SA)

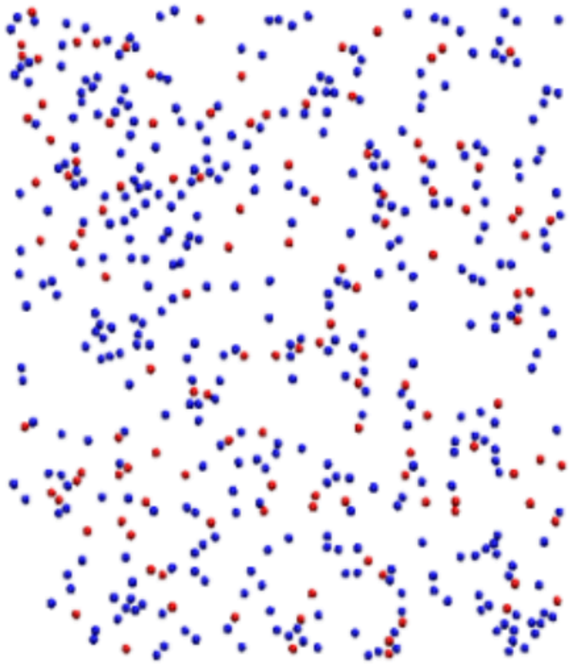

Dispersed particles

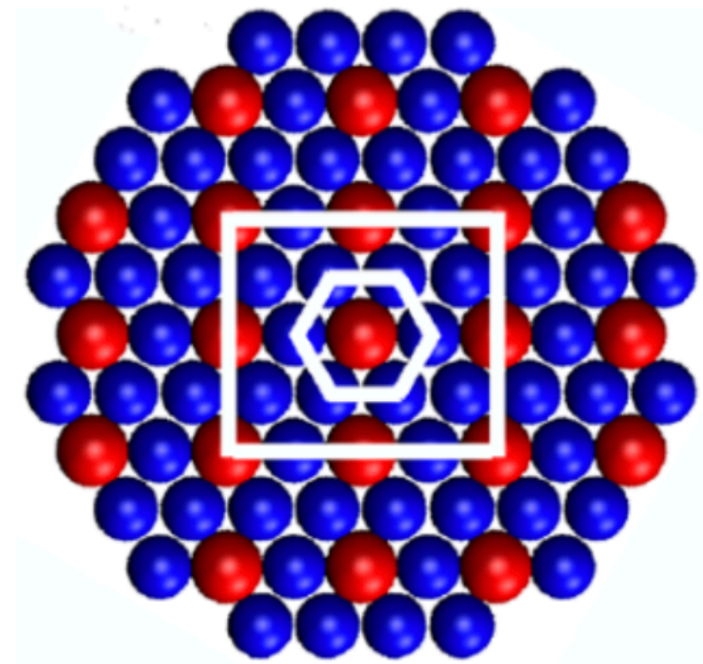

Ordered structure

Newsjournal of the Society for Industrial and Applied Mathematics sinews.siam.org

siam news

Volume 56/ Issue 6
July/August 2023

Self-assembly and Particle Aggregation in Stratified Fluids

Experimental Discovery and First-principle Mechanisms of Diffusion-induced Flows in Exterior Domains

By Roberto Camassa and Richard M. McLaughlin

The motion of particulates in the ocean as they fall under gravitation constitutes a critical component of the carbon cycle. Phytoplankton can photosynthesize dissolved carbon dioxide gas into dense, solid carbon debris called "marine snow," which facilitates the transport of carbon from the surface waters to the ocean depths. Over the course of eons, the carbon eventually turns into oil. The prevailing view maintains that particulate aggregation occurs through random turbulent oceanic motions that generate collisions between small-scale sticky particulates, which then form aggregates [4].

However, we recently discovered that such particles—when suspended at similar depths in stratified water—can slowly form aggregates in the absence of both external random flows and adhesion [7]. Surprisingly, these particles experience an effective horizontal attractive force that originates from the no-flux boundary condition. This attraction leads to self-assembly, during which particles form molecule-like assemblages that subsequently appear to dynamically solve jigsaw-like puzzles while en route to large-scale particulate discs.

Figure 1a depicts a time-series montage of the formation of a "particulate molecule" that eventually merges with a larger aggregate, and Figure 1b portrays a schematic of the experiment. Figures 1c and 1d present an initial image of the particulate distribution and a visual from 250 minutes later. Our findings offer insights into new mechanisms for large-scale aggregate formation in a wide variety of physical systems, including the ubiquitous stratified ocean waters, potential microplastic organization mechanisms, magnetic dynamos on Mercury and Ganymede, and even origin-of-life questions (such as matter's self-organization in deep ocean vents).

The discovery itself arose through a fortunate series of laboratory mistakes that ultimately led to a "eureka" moment. During a routine outreach demonstration, a setup error revealed this self-assembly phenomenon. Our demo—which seeks to exemplify

See **Particle Aggregation** *on page 3*

Figure 1. *Experimental self-assembly.* **1a.** *Time-series montage that illustrates the formation of a molecule. Five different output times—with 10 minutes between each instance—appear from left to right (artistic blurring depicts the motion). The spheres' radii and densities are respectively* 0.025-0.05 *cm and* 1.05 *g* cc^{-1}*; the top fluid is fresh water of density* 0.997 *g* cc^{-1} *and the bottom is a sodium chloride water solution of density* 1.1 *g* cc^{-1}*, with a transition thickness of approximately* 2 *cm.* **1b.** *Schematic of the experimental setup.* **1c.** *Initial cluster.* **1d.** *Final self-assembled cluster. Figure adapted from [7].*

Applications: Precision (sub nm scale) manufacturing of materials with advanced electrical, optical or magnetic properties

This talk: Two controlled colloidal SA case studies: (1) model-based, (2) data-driven

Colloidal SA Case Study 1: Model Based

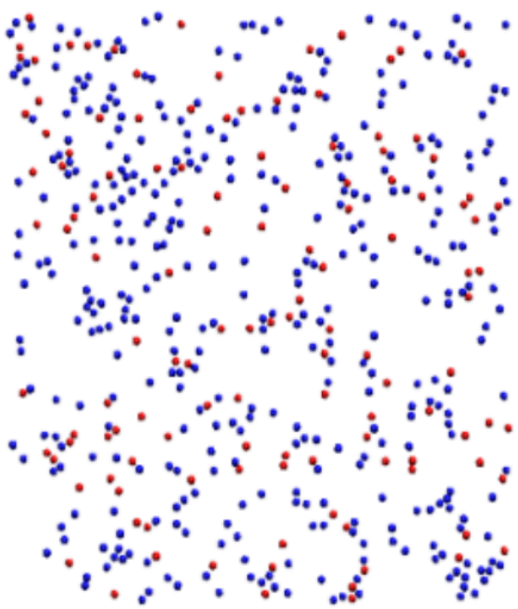

Dispersed particles

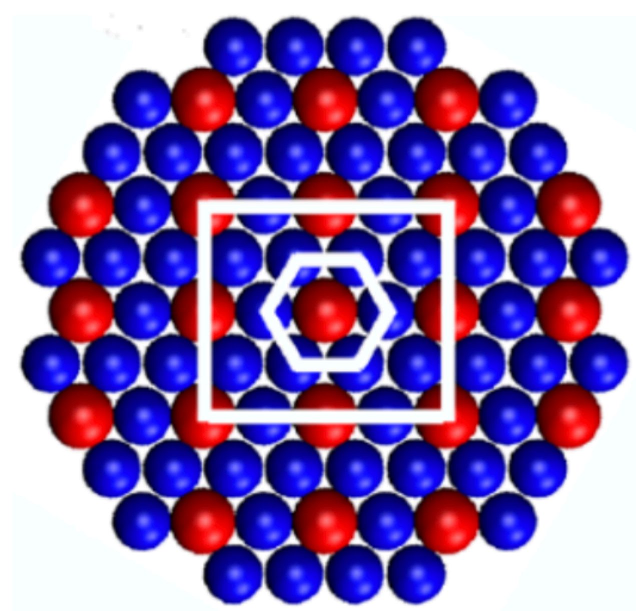

Ordered structure

Typical state: $\langle C_6 \rangle \in [0, 6]$

Averaged order parameter

Average number of hexagonally close-packed neighboring particles in 2D assembly

$\sim$ measure of crystallinity order

Typical control: u

Electric field voltage

Technical challenge:

Nonlinear + noisy molecular dynamics $\rightsquigarrow$ $\langle C_6 \rangle$ is a controlled stochastic process

Colloidal SA Case Study 2: Data Driven

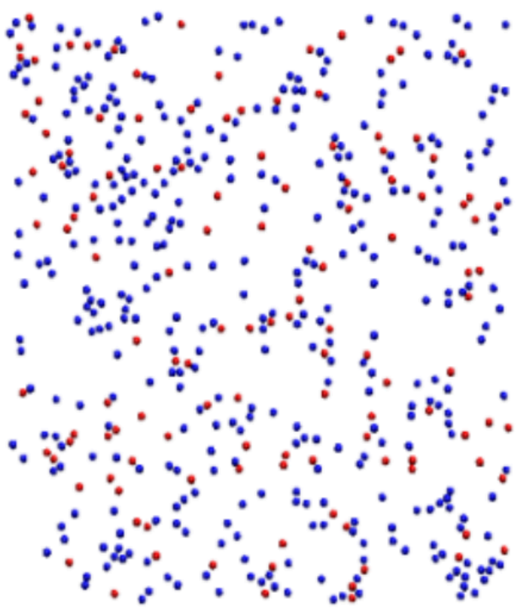

Dispersed particles

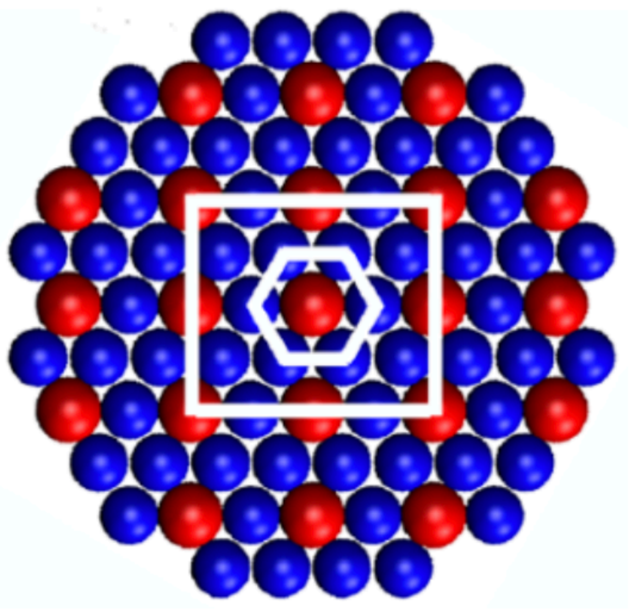

Ordered structure

Typical state: $(\langle C_{10}\rangle, \langle C_{12}\rangle) \in [0,1]^2$

Steinhart bond order parameters

useful for distinguishing between BCC and FCC structures

Typical control:

$(u_1, u_2) =$ (temperature, pressure)

Technical challenge:

Difficult to deduce first principle physics-based controlled dynamics over $(\langle C_{10}\rangle, \langle C_{12}\rangle)$

Controlled SA as Generalized Schrödinger Bridge

Intuition for Case Study 1: $\langle C_6 \rangle \approx 0$ ⇔ Crystalline disorder

$\langle C_6 \rangle \approx 6$ ⇔ Crystalline order

⇝ Steer the stochastic state $\langle C_6 \rangle$ from disordered at $t = 0$ to ordered at $t = T$

In typical applications, prescribed time horizon 200 s

Controlled SA as Generalized Schrödinger Bridge

Intuition for Case Study 1: $\langle C_6 \rangle \approx 0 \;\Leftrightarrow$ Crystalline disorder

$\langle C_6 \rangle \approx 6 \;\Leftrightarrow$ Crystalline order

⇝ Steer the stochastic state $\langle C_6 \rangle$ from disordered at $t = 0$ to ordered at $t = T$

In typical SA applications, prescribed time horizon 200 s

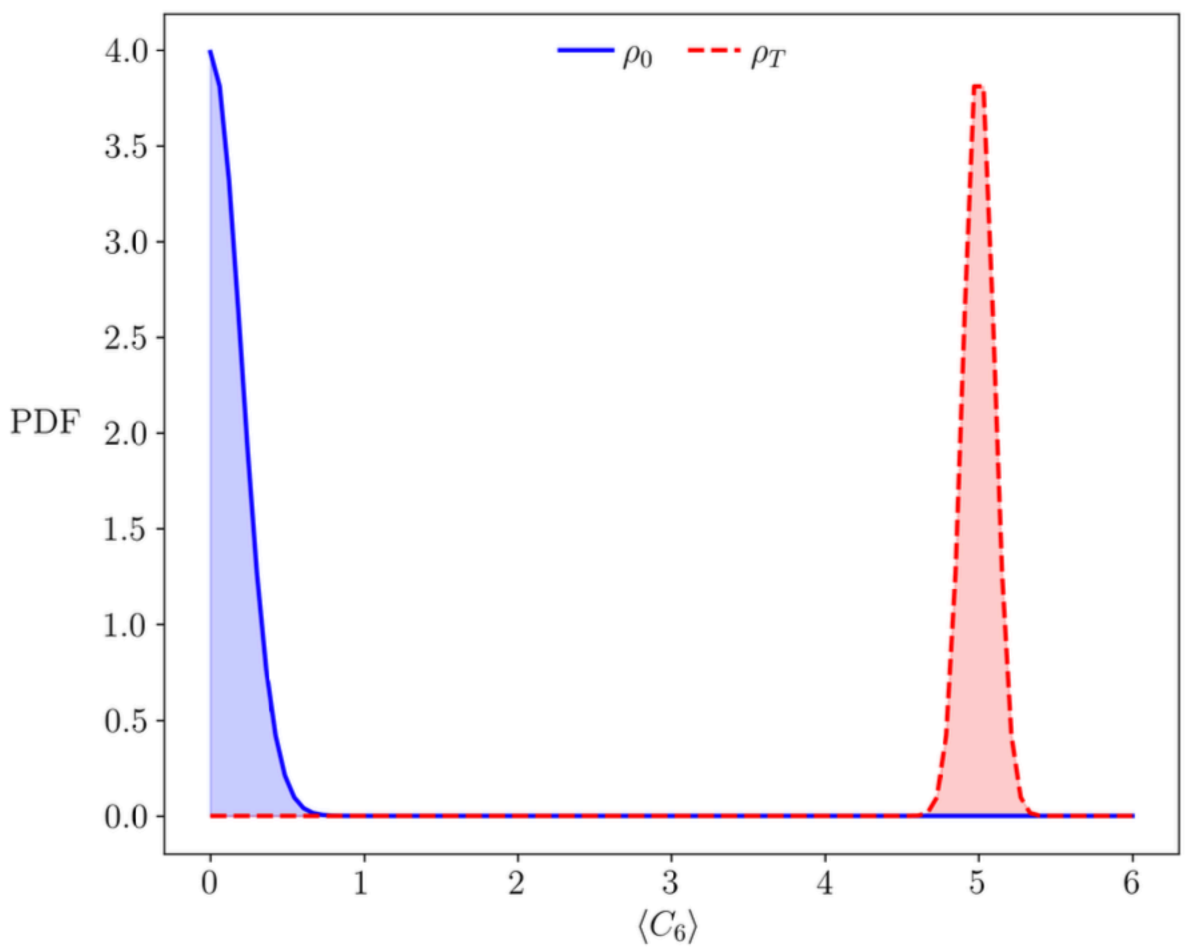

Endpoint PDF constraints:

$$\langle C_6 \rangle (t = 0) \sim \rho_0 \text{ given}$$
$$\langle C_6 \rangle (t = T) \sim \rho_T \text{ given}$$

Wanted control policy: $u = \pi(t, \langle C_6 \rangle)$

Minimum Effort Colloidal SA

Proposed formulation:

drift landscape, diffusion landscape, free energy landscape

$$\underbrace{D_1(x^u,u)}_{\text{drift landscape}} := \frac{\partial}{\partial x}\underbrace{D_2(x^u,u)}_{\text{diffusion landscape}} - \frac{\partial}{\partial x}\underbrace{F(x^u,u)}_{\text{free energy landscape}}\frac{D_2(x^u,u)}{k_B\theta}$$

either from model or learnt from MD simulation data

$$\inf_{u\in\mathcal{U}} \quad \mathbb{E}_{\mu^u}\left[\int_0^T \frac{1}{2}u^2 \,\mathrm{d}t\right],$$

subject to $\underbrace{\mathrm{d}x^u}_{\langle C_6\rangle} = D_1(x^u,u)\,\mathrm{d}t + \sqrt{2D_2(x^u,u)}\,\underbrace{\mathrm{d}w}_{\text{standard Wiener process}},$

$$x^u(t=0) \sim \mathrm{d}\mu_0 = \rho_0\,\mathrm{d}x^u, \quad x^u(t=T) \sim \mathrm{d}\mu_T = \rho_T\,\mathrm{d}x^u$$

Minimum Effort Colloidal SA

Equivalent formulation:

Guaranteed existence-uniqueness for compactly supported ρ_0, ρ_T

$$\inf_{(\rho^u,u)} \int_0^T \int_{\mathbb{R}} \frac{1}{2} u^2(x^u,t)\,\rho^u(x^u,t)\,\mathrm{d}x^u\,\mathrm{d}t$$

subject to $$\frac{\partial \rho^u}{\partial t} = -\frac{\partial}{\partial x^u}\left(D_1\rho^u\right) + \frac{\partial^2}{\partial x^{u2}}\left(D_2\rho^u\right)$$

$$\rho^u(x^u,t=0) = \rho_0, \quad \rho^u(x^u,t=T) = \rho_T$$

Controlled Fokker-Planck-Kolmogorov PDE

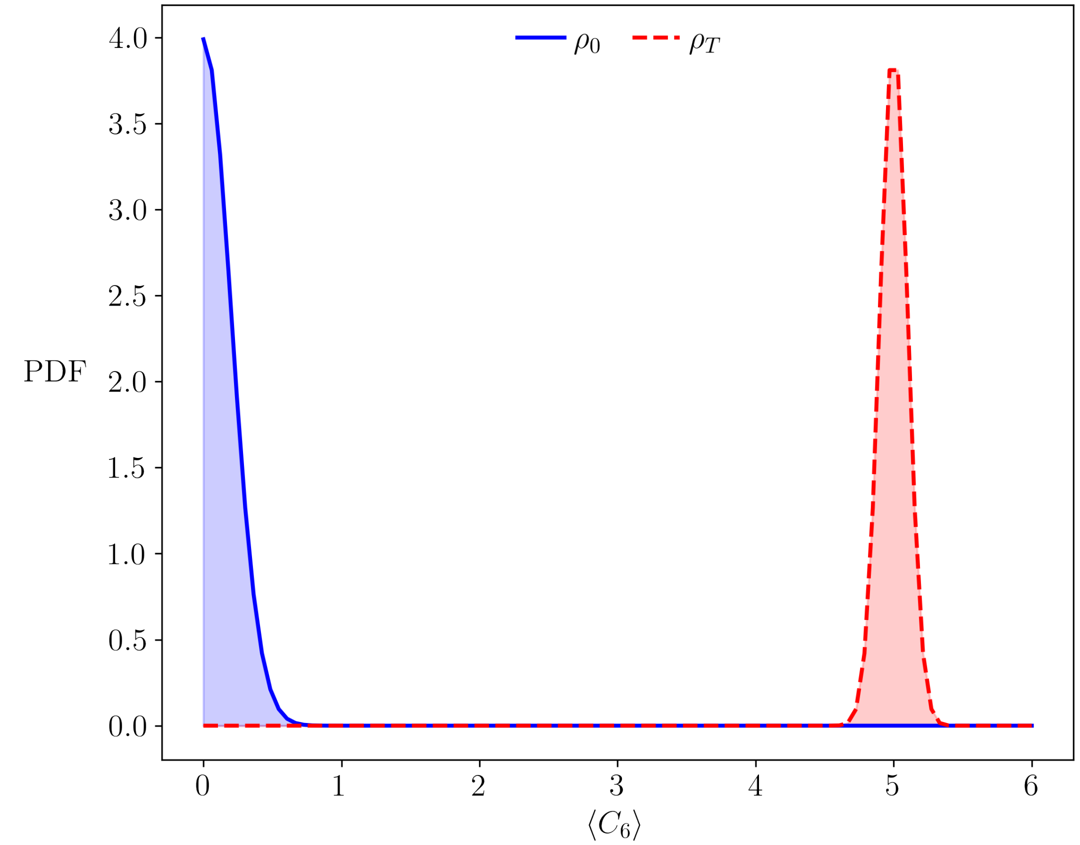

Generalized Schrödinger Bridge Problem (GSBP)

Classical SBP: $D_1 \equiv u, \quad D_2 \equiv \text{Identity}$

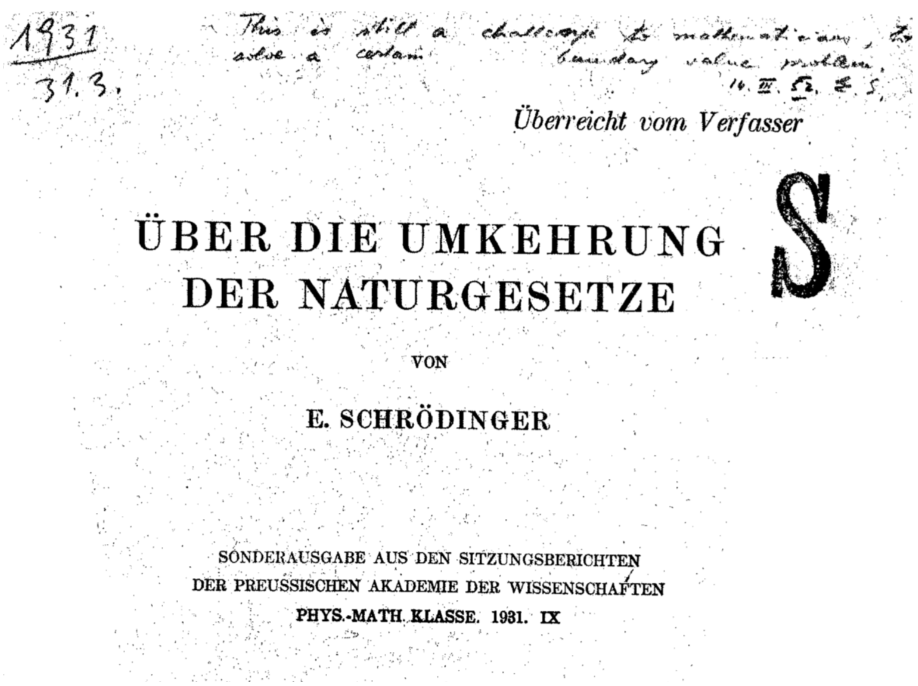
1931
31.3.
This is still a challenge to mathematicians, to solve a certain boundary value problem. 14.III.52. E.S.

Überreicht vom Verfasser

ÜBER DIE UMKEHRUNG DER NATURGESETZE

VON

E. SCHRÖDINGER

SONDERAUSGABE AUS DEN SITZUNGSBERICHTEN DER PREUSSISCHEN AKADEMIE DER WISSENSCHAFTEN PHYS.-MATH. KLASSE. 1931. IX

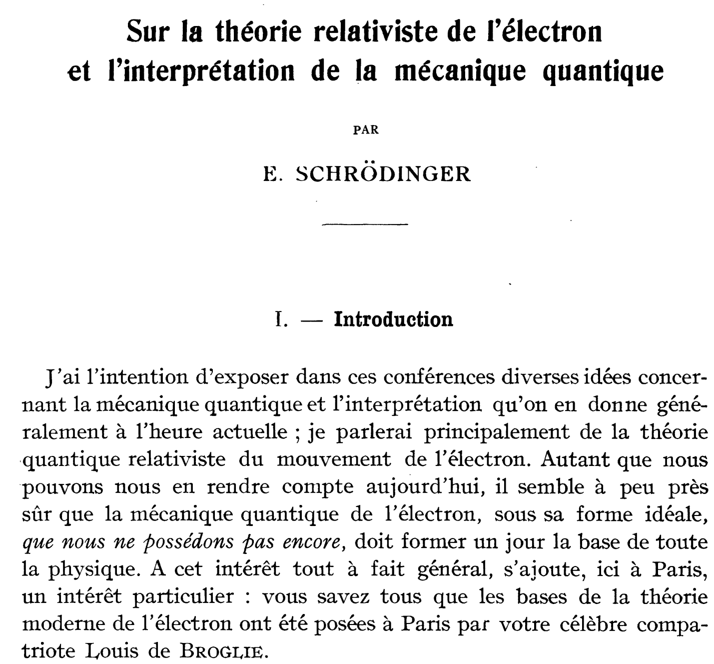
Sur la théorie relativiste de l'électron et l'interprétation de la mécanique quantique

PAR

E. SCHRÖDINGER

I. — **Introduction**

J'ai l'intention d'exposer dans ces conférences diverses idées concernant la mécanique quantique et l'interprétation qu'on en donne généralement à l'heure actuelle ; je parlerai principalement de la théorie quantique relativiste du mouvement de l'électron. Autant que nous pouvons nous en rendre compte aujourd'hui, il semble à peu près sûr que la mécanique quantique de l'électron, sous sa forme idéale, *que nous ne possédons pas encore*, doit former un jour la base de toute la physique. A cet intérêt tout à fait général, s'ajoute, ici à Paris, un intérêt particulier : vous savez tous que les bases de la théorie moderne de l'électron ont été posées à Paris par votre célèbre compatriote Louis de Broglie.

Classical SBP ≡ Stochastic version of dynamic OMT

Minimum effort ≡ Most likely evolution between observed distributions

Generalized Schrödinger Bridge Problem (GSBP)

Classical SBP: $D_1 \equiv u, \quad D_2 \equiv \text{Identity}$

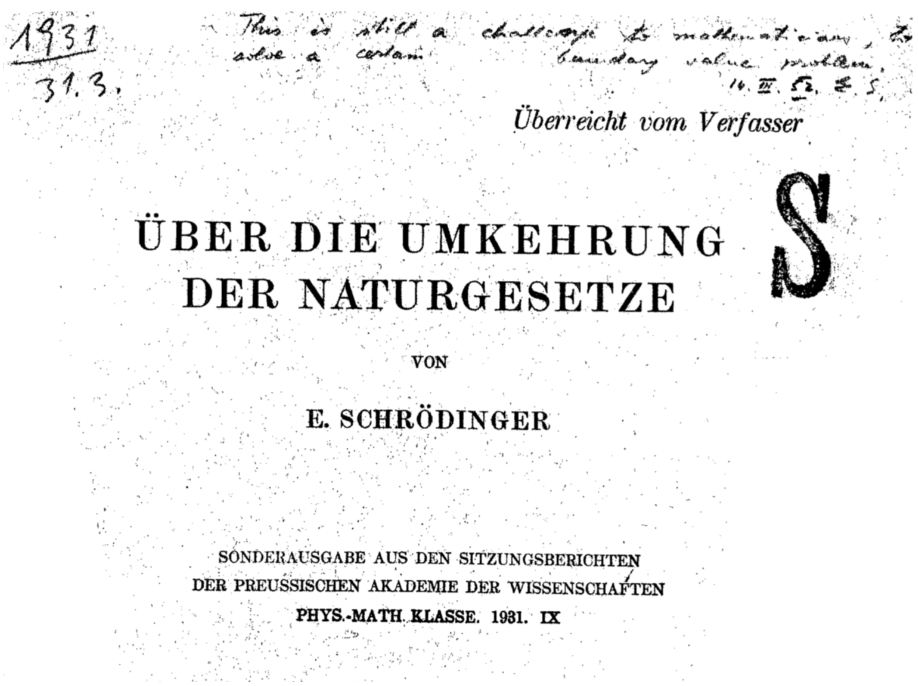

1931
31.3.
This is still a challenge to mathematicians, to solve a certain boundary value problem. 14.III.52 E.S.

Überreicht vom Verfasser

S

ÜBER DIE UMKEHRUNG
DER NATURGESETZE

VON

E. SCHRÖDINGER

SONDERAUSGABE AUS DEN SITZUNGSBERICHTEN
DER PREUSSISCHEN AKADEMIE DER WISSENSCHAFTEN
PHYS.-MATH. KLASSE. 1931. IX

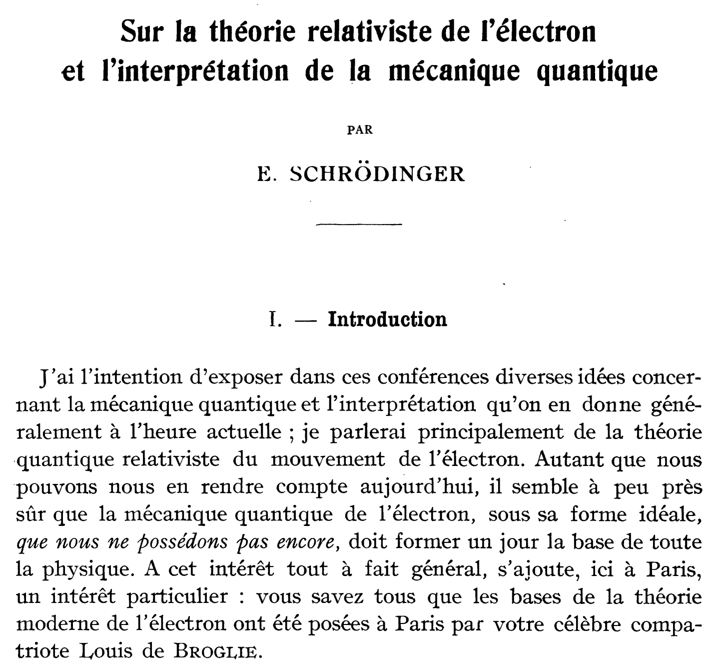

Sur la théorie relativiste de l'électron
et l'interprétation de la mécanique quantique

PAR

E. SCHRÖDINGER

I. — **Introduction**

J'ai l'intention d'exposer dans ces conférences diverses idées concernant la mécanique quantique et l'interprétation qu'on en donne généralement à l'heure actuelle ; je parlerai principalement de la théorie quantique relativiste du mouvement de l'électron. Autant que nous pouvons nous en rendre compte aujourd'hui, il semble à peu près sûr que la mécanique quantique de l'électron, sous sa forme idéale, *que nous ne possédons pas encore*, doit former un jour la base de toute la physique. A cet intérêt tout à fait général, s'ajoute, ici à Paris, un intérêt particulier : vous savez tous que les bases de la théorie moderne de l'électron ont été posées à Paris par votre célèbre compatriote Louis de Broglie.

Classical SBP ≡ Stochastic version of dynamic OMT

Minimum effort ≡ Most likely evolution between observed distributions

In our colloidal SA:

Both D_1, D_2 are nonlinear in state + non-affine in control

Conditions for Optimality: Case 1

Three coupled PDEs with endpoint boundary conditions:

$$\frac{\partial \psi}{\partial t} = \frac{1}{2}\left(\pi^{\text{opt}}\right)^2 - \frac{\partial \psi}{\partial x} D_1 - \frac{\partial^2 \psi}{\partial x^{u2}} D_2$$ **HJB PDE**

$$\frac{\partial \rho^u}{\partial t} = -\frac{\partial}{\partial x^u}\left(D_1 \rho^u\right) + \frac{\partial^2}{\partial x^{u2}}\left(D_2 \rho^u\right)$$ **Controlled FPK PDE**

$$\pi^{\text{opt}}(x^u, t) = \frac{\partial \psi}{\partial x^u}\frac{\partial D_1}{\partial u} + \frac{\partial^2 \psi}{\partial x^{u2}}\frac{\partial D_2}{\partial u}$$ **Optimal policy**

$$\rho^u(x^u, t=0) = \rho_0, \quad \rho^u(x^u, t=T) = \rho_T$$ **Boundary conditions**

value function	optimally controlled PDF	optimal policy

to be solved for the triple: $\psi\left(x^u, t\right)$, $\rho^u\left(x^u, t\right)$, $\pi^{\text{opt}}\left(x^u, t\right)$

Conditions for Optimality: Case 1

Three coupled PDEs with endpoint boundary conditions:

$$\frac{\partial \psi}{\partial t} = \frac{1}{2}\left(\pi^{\mathrm{opt}}\right)^2 - \frac{\partial \psi}{\partial x} D_1 - \frac{\partial^2 \psi}{\partial x^{u2}} D_2$$

HJB PDE

$$\frac{\partial \rho^u}{\partial t} = -\frac{\partial}{\partial x^u}\left(D_1 \rho^u\right) + \frac{\partial^2}{\partial x^{u2}}\left(D_2 \rho^u\right)$$

Controlled FPK PDE

$$\pi^{\mathrm{opt}}(x^u, t) = \frac{\partial \psi}{\partial x^u}\frac{\partial D_1}{\partial u} + \frac{\partial^2 \psi}{\partial x^{u2}}\frac{\partial D_2}{\partial u}$$

Optimal policy

$$\rho^u(x^u, t=0) = \rho_0, \quad \rho^u(x^u, t=T) = \rho_T$$

Boundary conditions

value function	optimally controlled PDF	optimal policy
$\psi\left(x^u, t\right)$	$\rho^u\left(x^u, t\right)$	$\pi^{\mathrm{opt}}\left(x^u, t\right)$

to be solved for the triple: $\psi\left(x^u, t\right)$, $\rho^u\left(x^u, t\right)$, $\pi^{\mathrm{opt}}\left(x^u, t\right)$

Cf. classical SBP: two coupled PDEs + optimal policy explicit in value fn ψ

Idea: Train Physics Informed Neural Network (PINN) to Learn the Solution of the GSBP

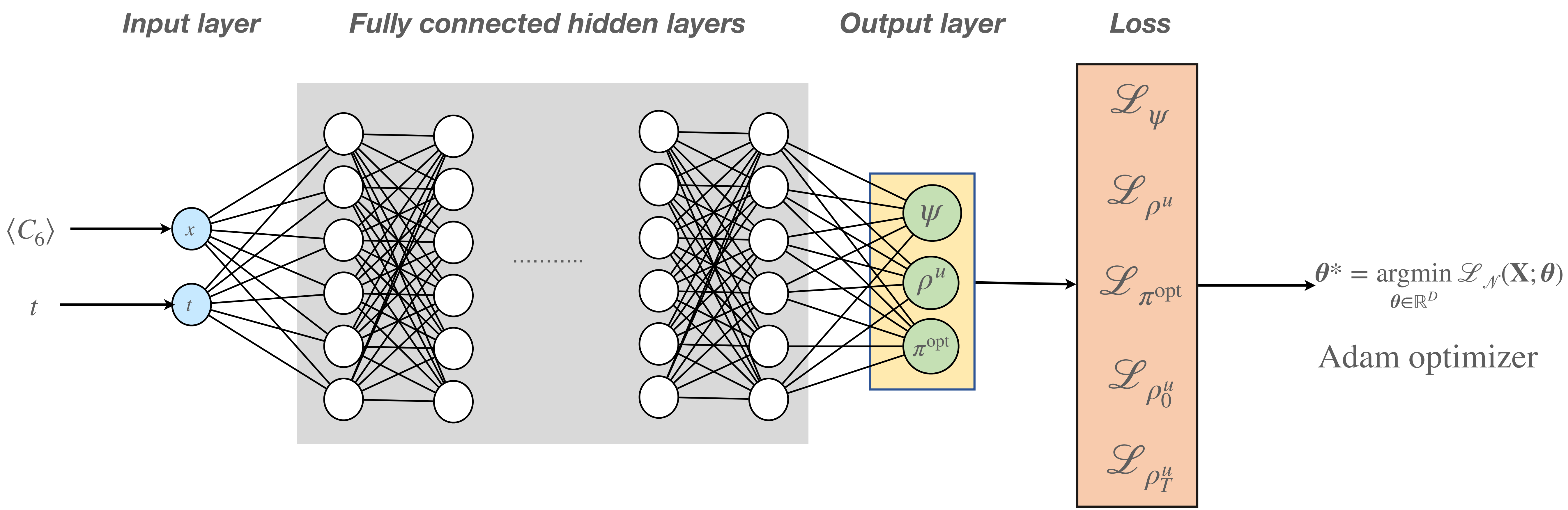

$$\mathscr{L}_{\mathcal{N}} = \mathscr{L}_\psi + \mathscr{L}_{\rho^u} + \mathscr{L}_{\pi^{\text{opt}}} + \mathscr{L}_{\rho_0^u} + \mathscr{L}_{\rho_T^u}$$

[Lu Lu et al, 2021] [Niaki et al, 2021]

Case Study 1: Residuals for PINN Training

Benchmark controlled self-assembly system: [Y Xue, et al, *IEEE Trans. Control Sys. Technology*, 2014]

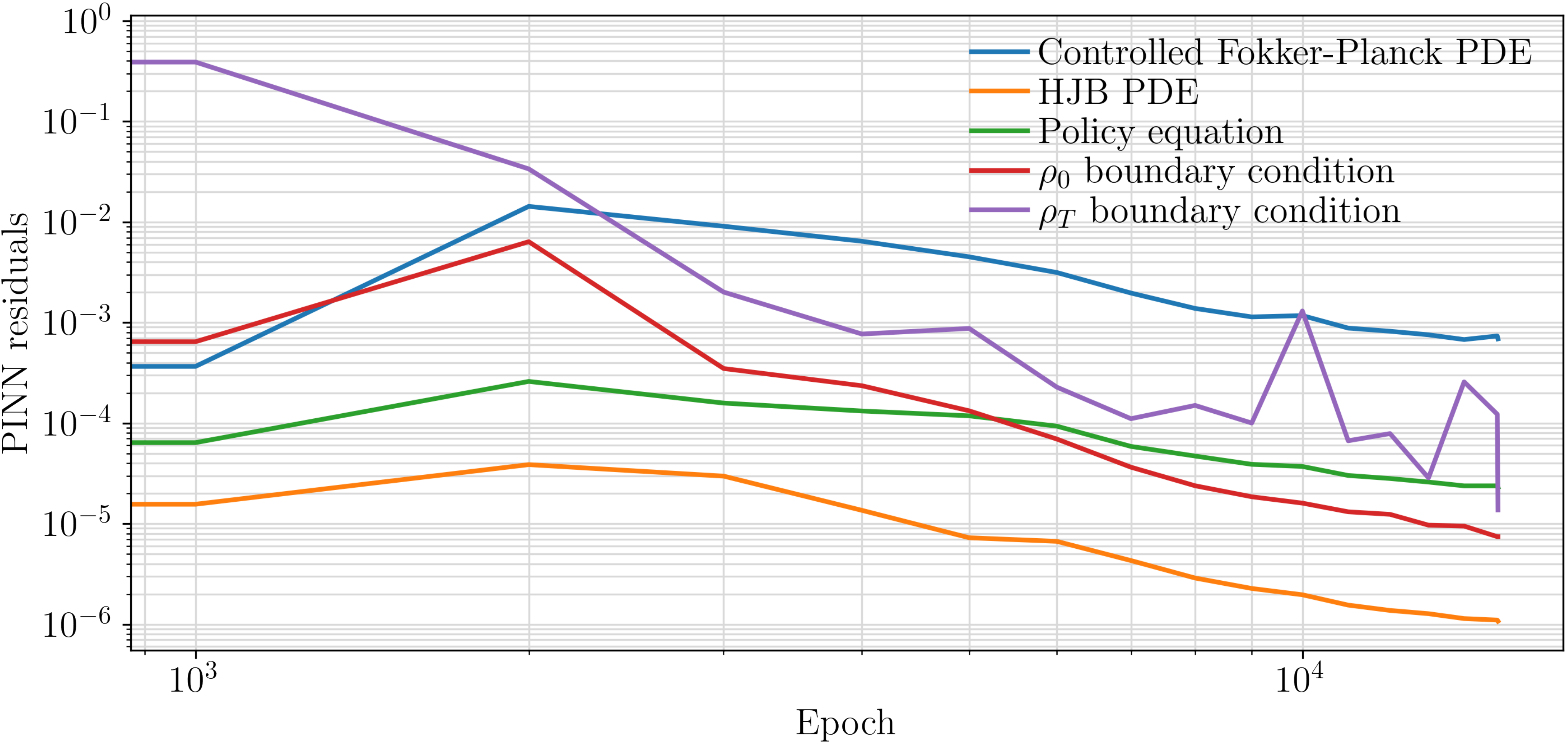

Case Study 1: Optimal Policy

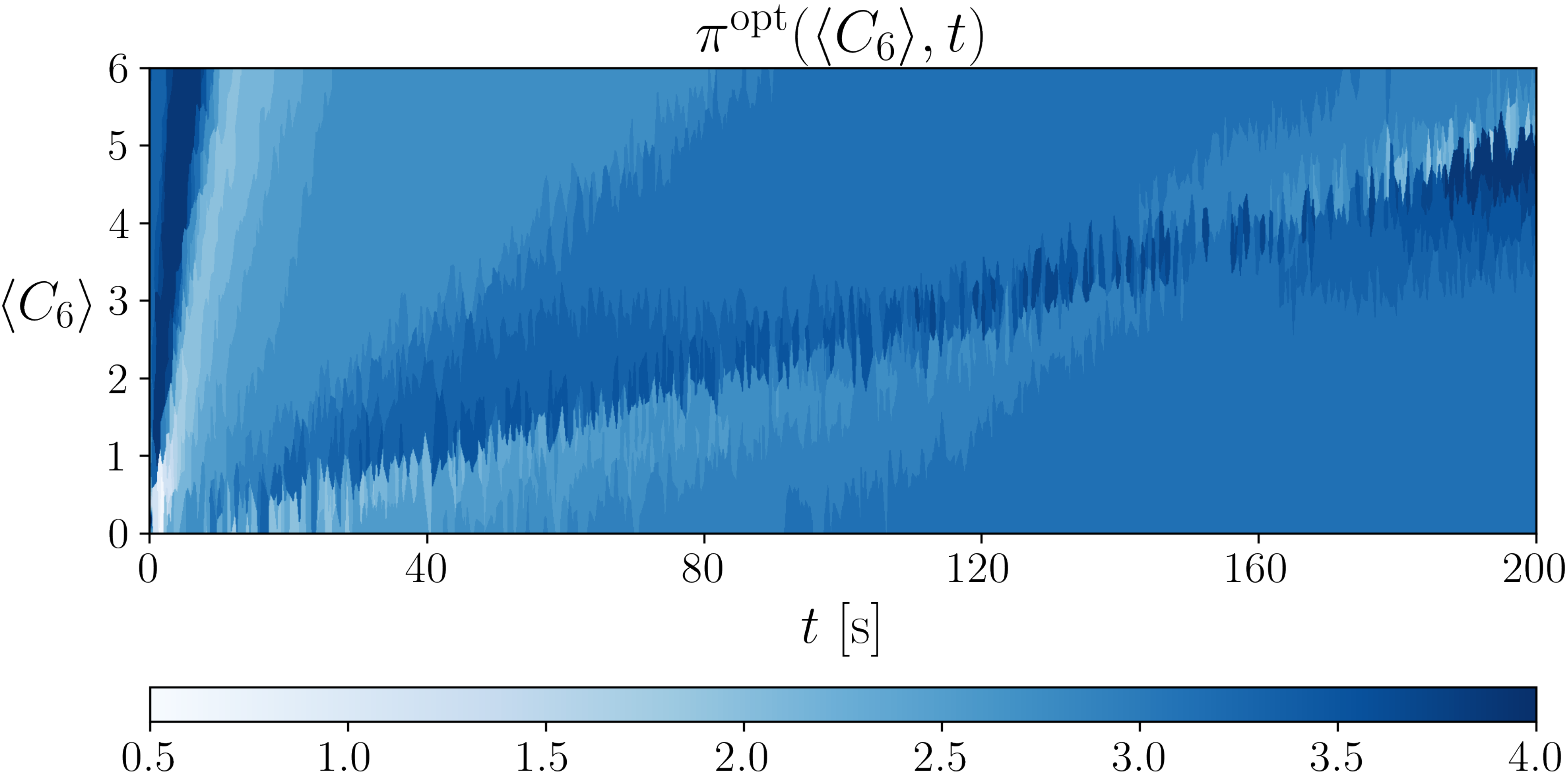

Case Study 1: Value Function

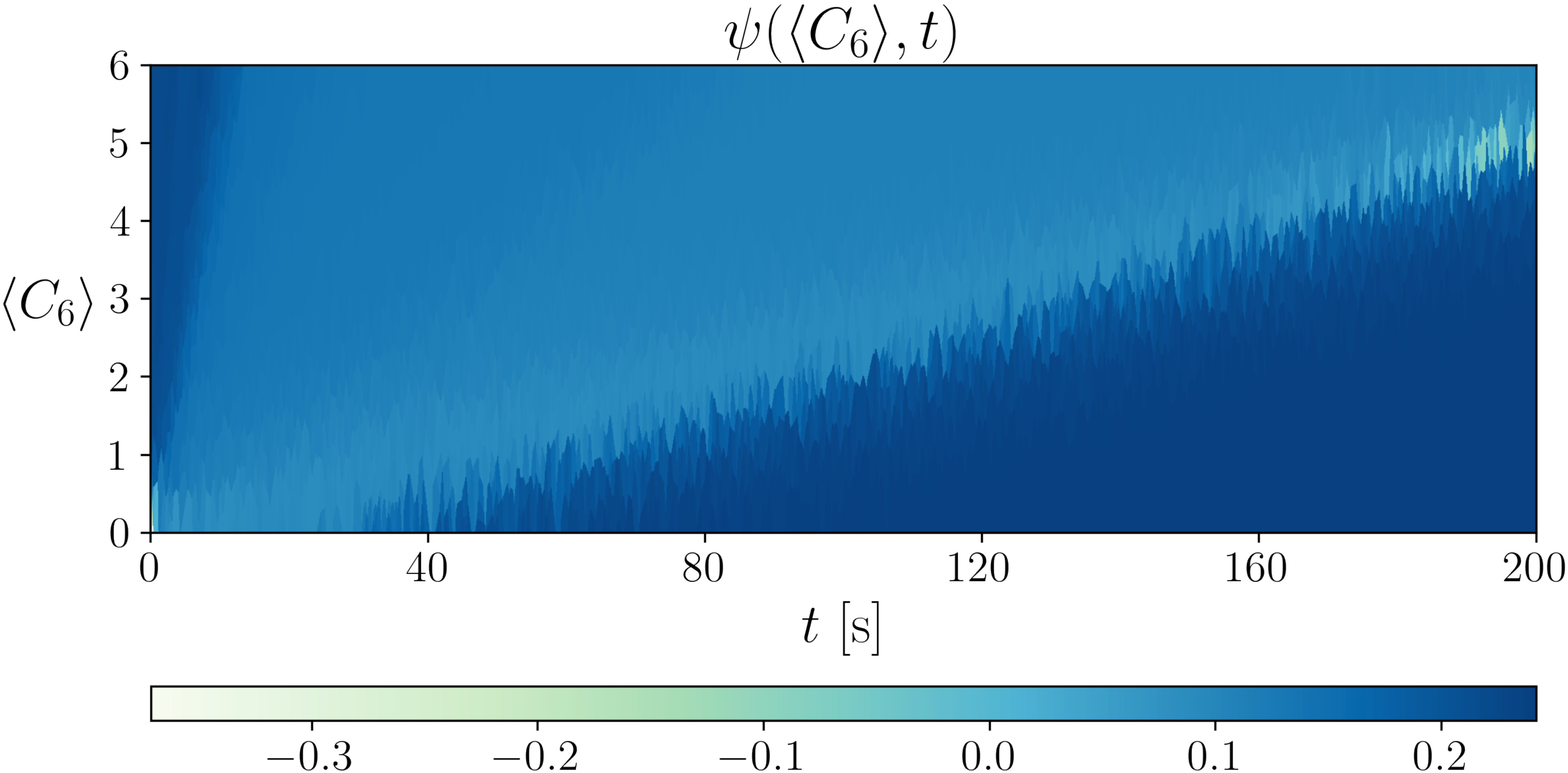

Case Study 1: Optimally Controlled State PDFs

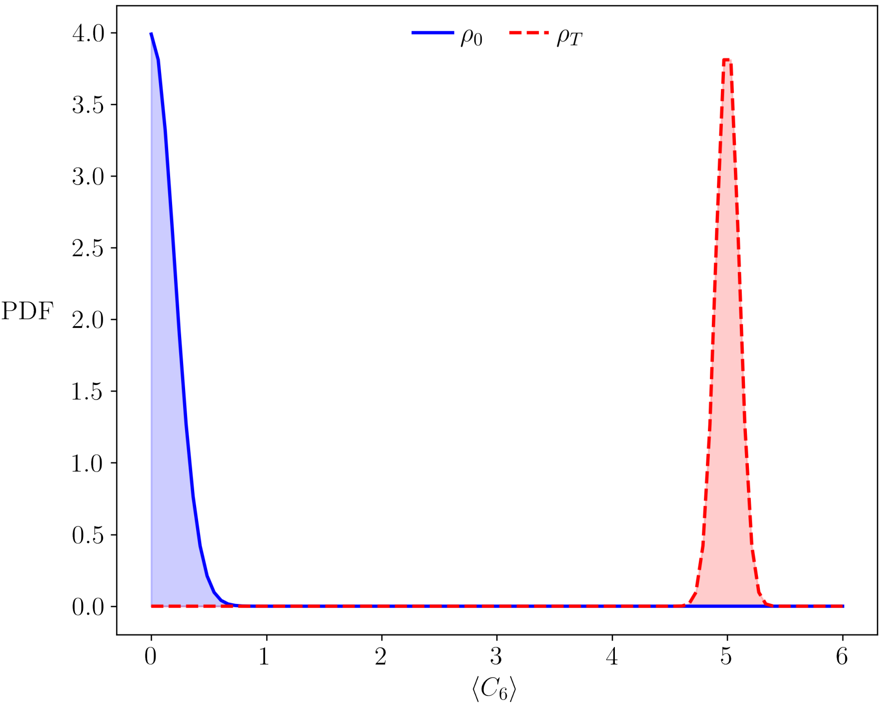

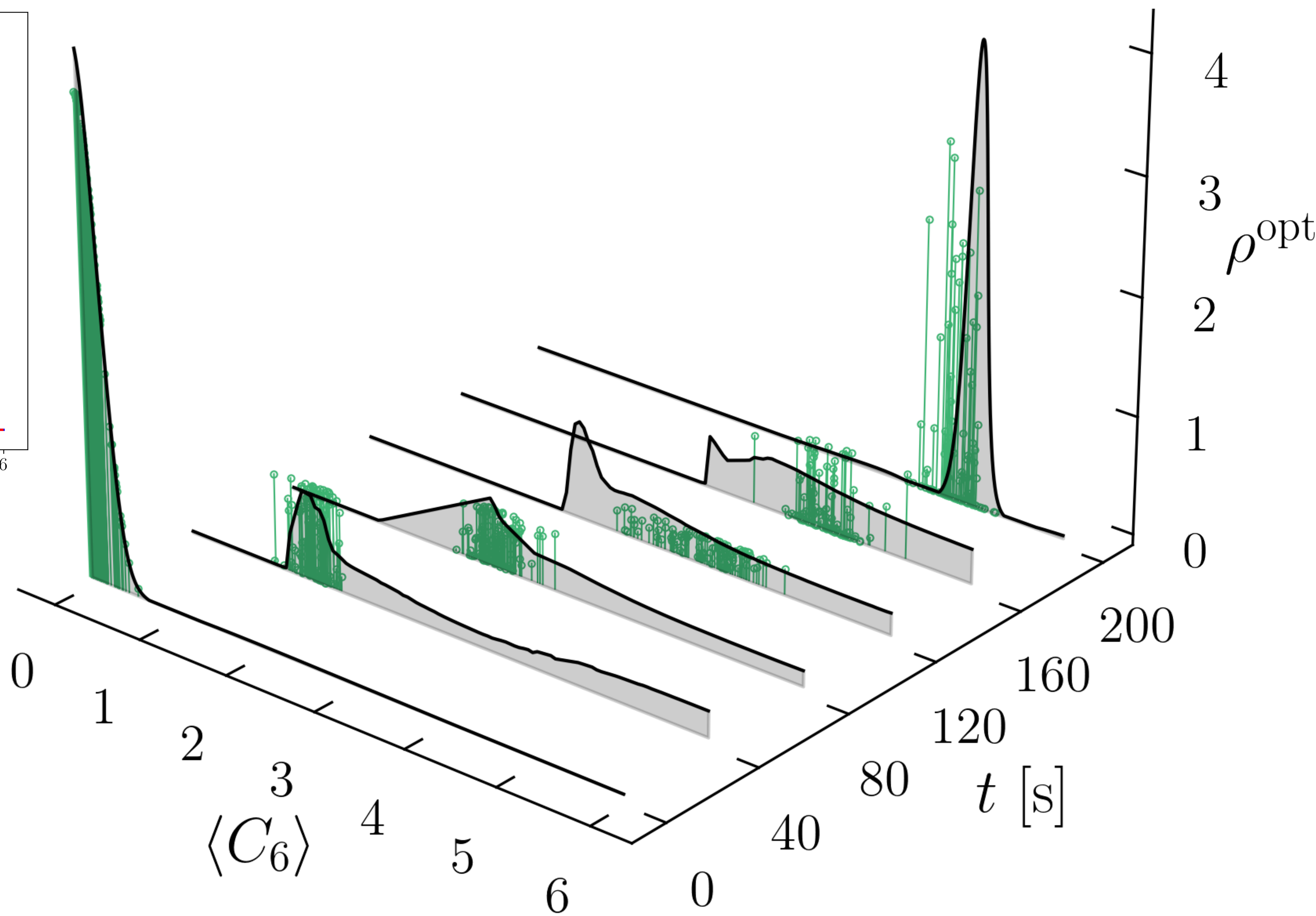

… the MSE losses are not appropriate for enforcing the endpoint PDF constraints

Case Study 1: Closed Loop Sample Paths

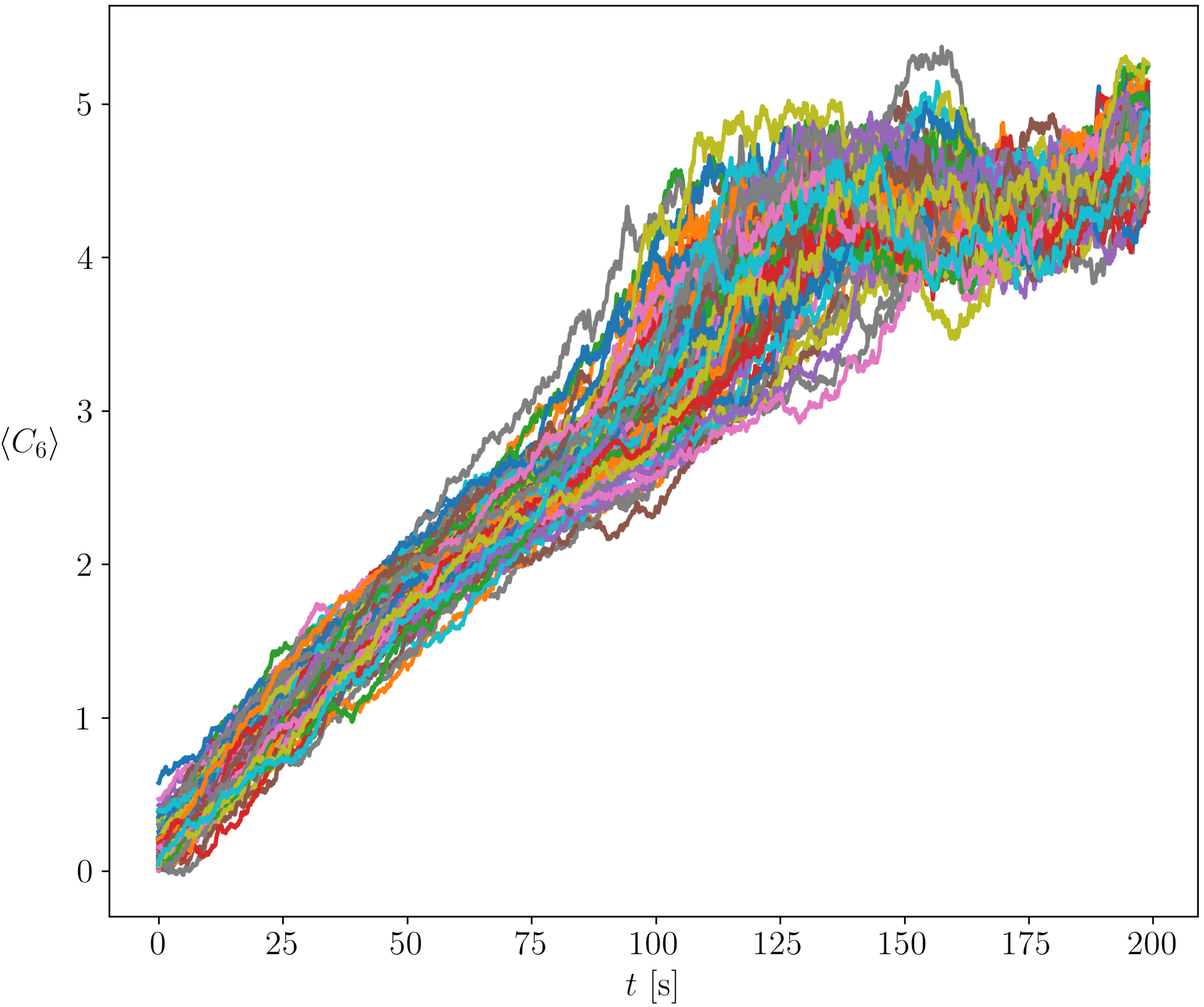

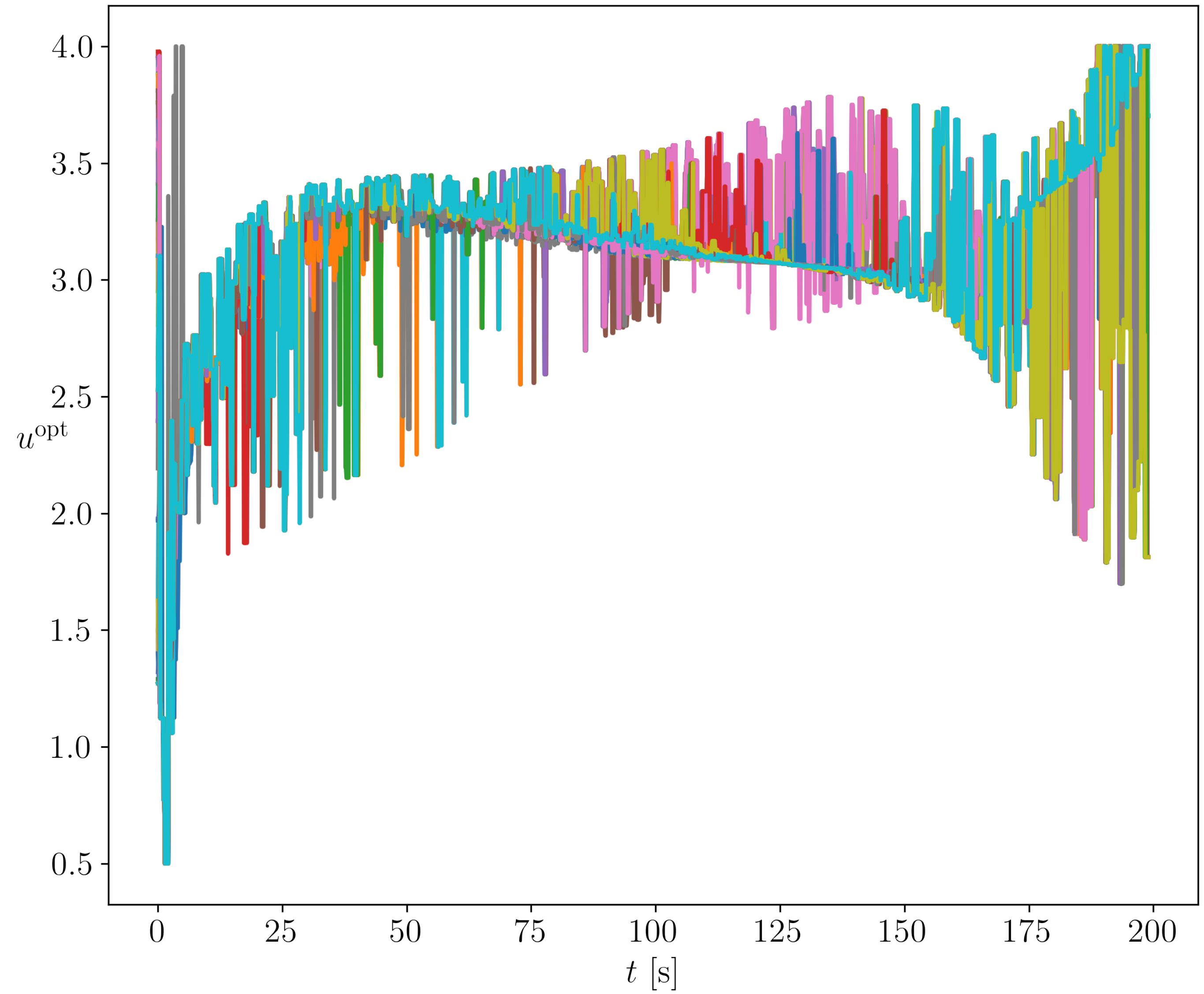

GSBP Conditions for Optimality with m Inputs

$m+2$ coupled PDEs with endpoint boundary conditions:

Drift coefficient   Diffusion tensor

$$\frac{\partial \psi}{\partial t} = \frac{1}{2}\|\boldsymbol{u}_{\text{opt}}\|_2^2 - \langle \nabla_{\boldsymbol{x}}\psi, \boldsymbol{f}\rangle - \langle \boldsymbol{G}, \mathbf{Hess}(\psi)\rangle,$$

$$\frac{\partial \rho_{\text{opt}}^{\boldsymbol{u}}}{\partial t} = -\nabla.(\rho_{\text{opt}}^{\boldsymbol{u}}\boldsymbol{f}) + \langle \boldsymbol{G}, \mathbf{Hess}(\rho_{\text{opt}}^{\boldsymbol{u}})\rangle,$$

$$\boldsymbol{u}_{\text{opt}} = \nabla_{\boldsymbol{u}_{\text{opt}}}\left(\langle \nabla_{\boldsymbol{x}}\psi, \boldsymbol{f}\rangle + \langle \boldsymbol{G}, \mathbf{Hess}(\psi)\rangle\right),$$

$$\rho_{\text{opt}}^{\boldsymbol{u}}(0,\boldsymbol{x}) = \rho_0, \qquad \rho_{\text{opt}}^{\boldsymbol{u}}(T,\boldsymbol{x}) = \rho_T,$$

Cf. classical SBP: two coupled PDEs + optimal policy explicit in value fn ψ

Data-driven GSBP for Colloidal SA

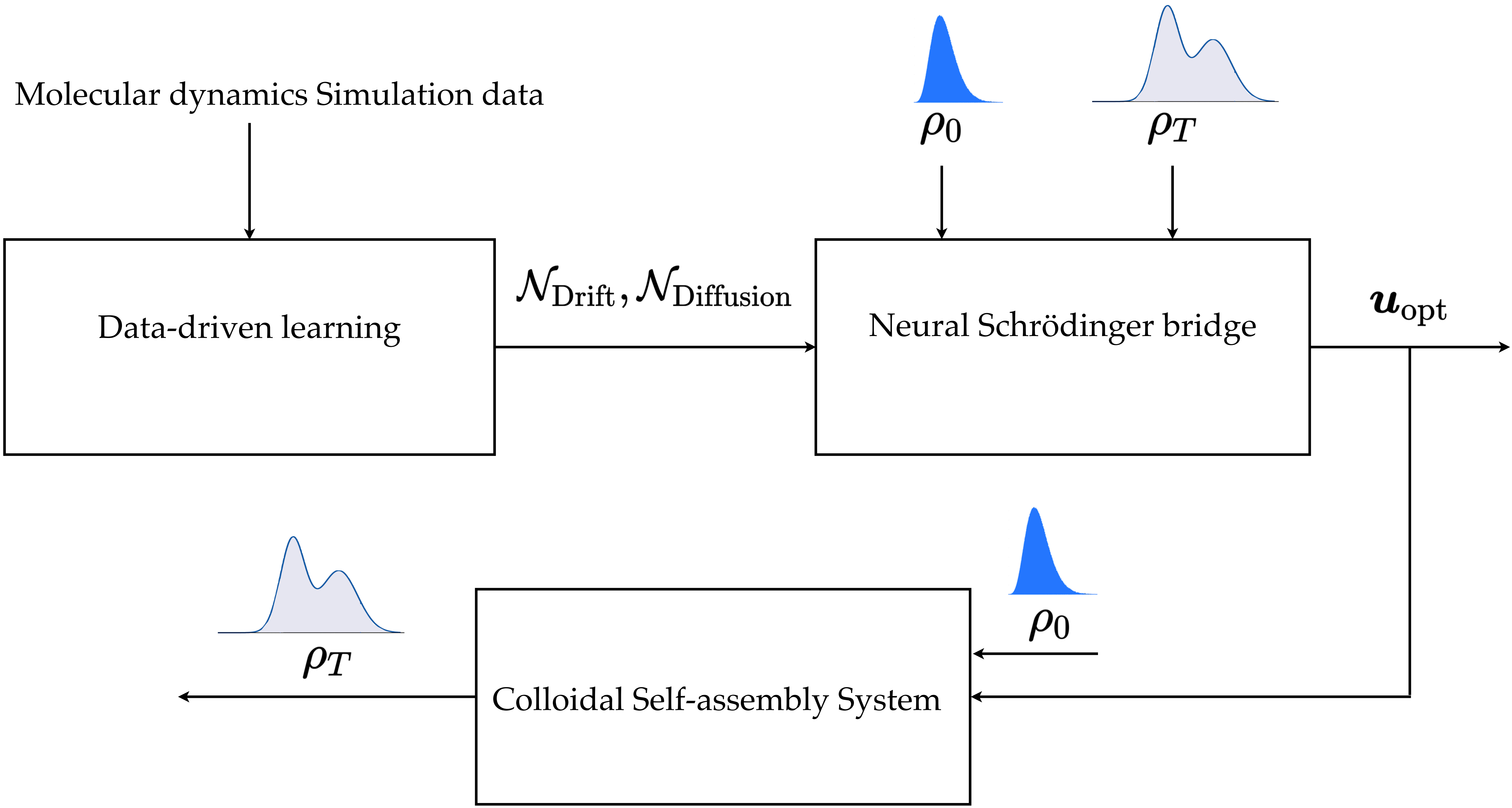

Architecture for Data-driven GSBP

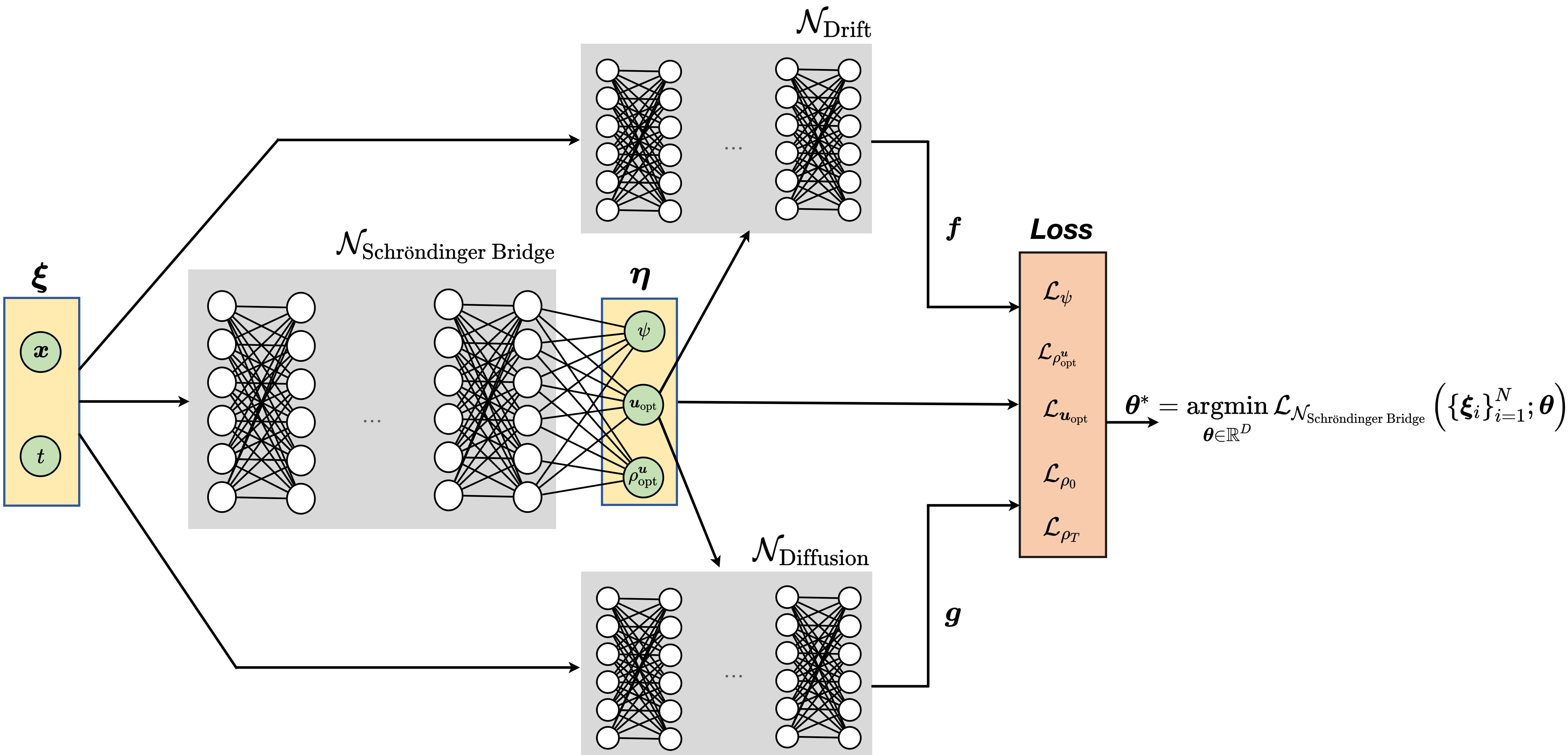

Sinkhorn Losses for Boundary Conditions

$$W_{\varepsilon}^{2}(\mu_0,\mu_1) := \inf_{\pi\in\Pi_2(\mu_0,\mu_T)} \int_{\mathbb{R}^n\times\mathbb{R}^n} \{\|\boldsymbol{x}-\boldsymbol{y}\|_2^2 + \varepsilon\log\pi(\boldsymbol{x},\boldsymbol{y})\}\mathrm{d}\pi(\boldsymbol{x},\boldsymbol{y})$$

For boundary conditions, use Sinkhorn losses: $\mathcal{L}_{\rho_i} := W_{\varepsilon}^{2}\left(\rho_i, \rho_i^{\text{epoch index}}(\boldsymbol{\theta})\right)$

Implementation friendly for PINN training:

$$\texttt{Autodiff}_{\boldsymbol{\theta}} W_{\varepsilon}^{2}\left(\rho_i, \rho_i^{\text{epoch index}}(\boldsymbol{\theta})\right) \quad \forall i \in \{0, T\}$$

Case Study 2: Synthesize BCC Crystalline Structure by PDF Steering in $\left(\langle C_{10}\rangle, \langle C_{12}\rangle\right)$ Space

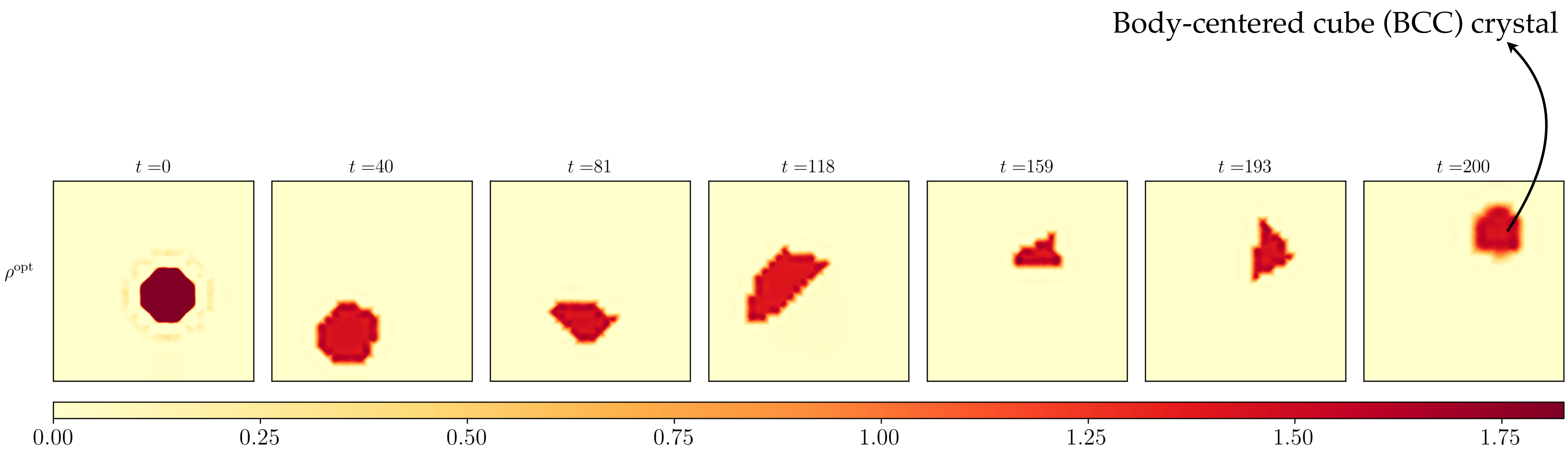

Data-driven:

Uses PINN with Sinkhorn losses + the drift-diffusion are themselves NNs

Case Study 2: Closed Loop State Sample Paths

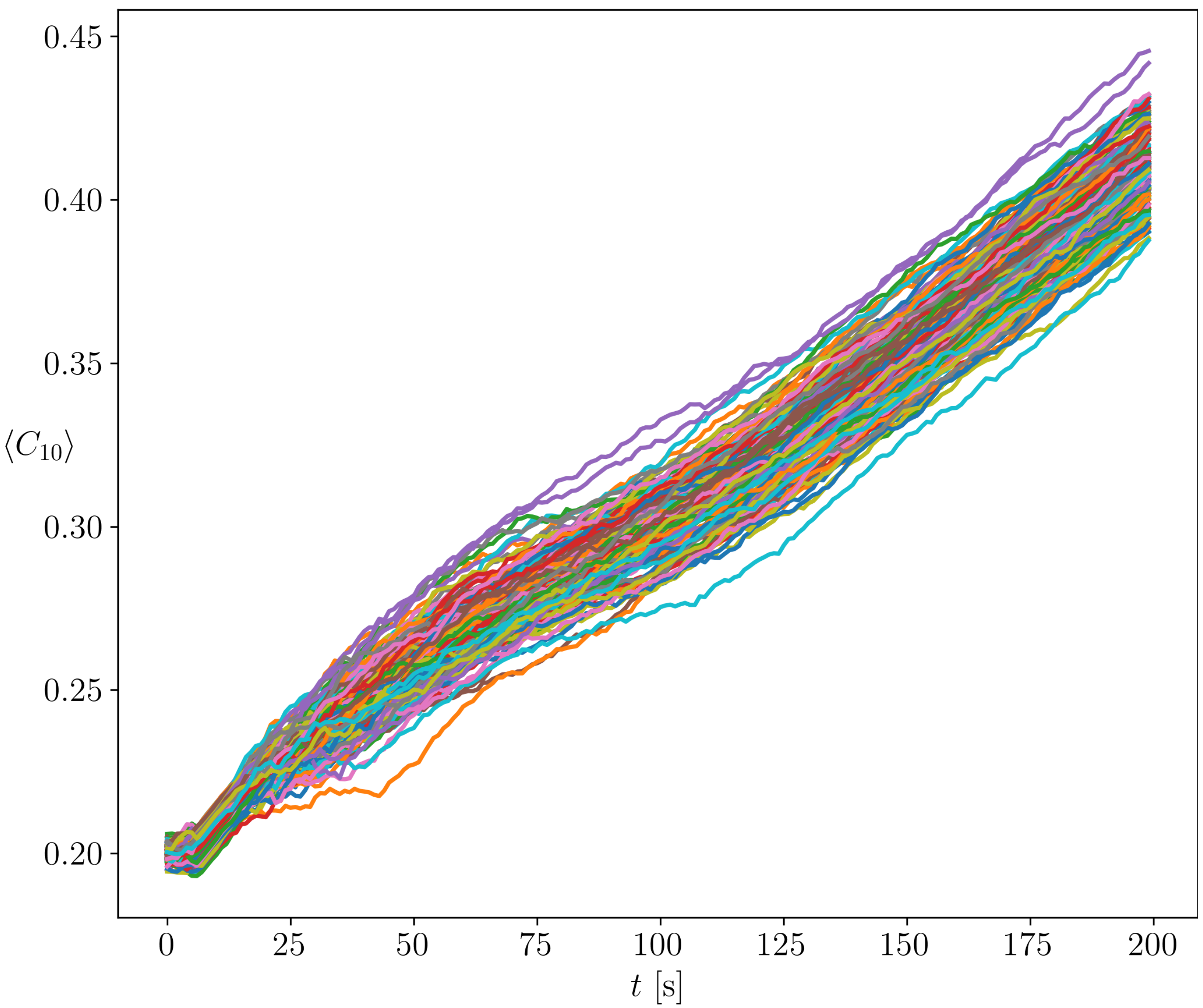

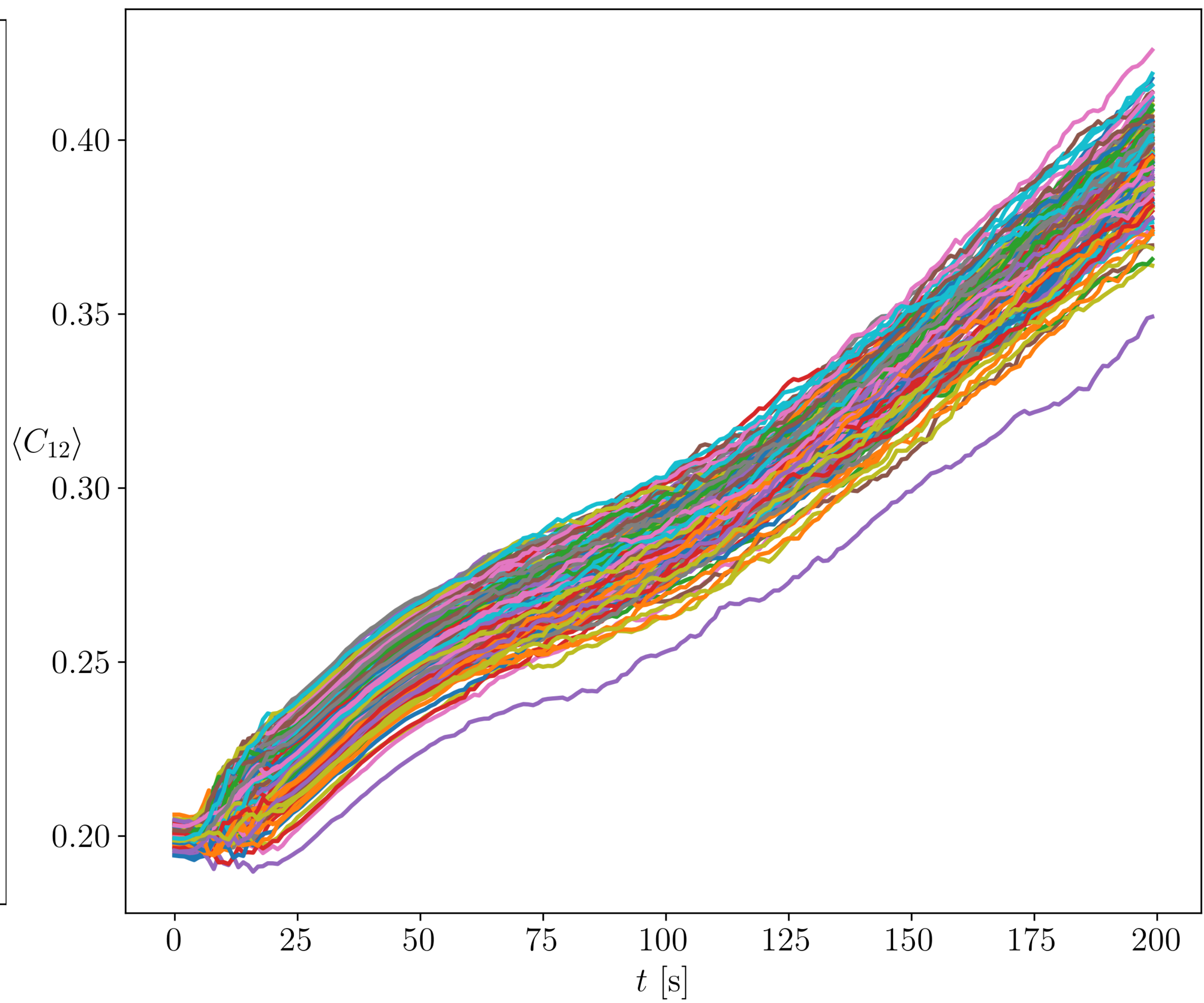

Desired transport from mean (0.2, 0.2) to (0.40,0.37) for BCC structure

Take Home Message

GSBPs arise quite naturally in engineering applications such as colloidal SA

Computational methods for GSBPs need more development

Refs for this work:

I. Nodozi, J. O'Leary, A. Mesbah, A.H., A physics-informed deep learning approach for minimum effort stochastic control of colloidal self-assembly, *ACC 2023*

I. Nodozi, C. Yan, M. Khare, A.H., A. Mesbah, Neural Schrödinger Bridge with Sinkhorn Losses: Application to Data-driven Minimum Effort Control of Colloidal Self-assembly, *arXiv????*

Thank You

Acknowledgement: NSF **CMMI 2112755**